Room-Temperature Photogeneration of Nitrosyl Linkage Isomers in Ruthenium Nitrosyl Complexes

Artem Mikhailov, Emmanuel Wenger, Gennadiy A Kostin, Dominik Schaniel

Room-temperature photogeneration of nitrosyl linkage isomers in ruthenium nitrosyl complexes

A.A. Mikhailov,[a,b] E. Wenger, [c] G.A. Kostin,[a,b] and D. Schaniel[c]

[a] A.A. Mikhailov and Prof. G.A. Kostin
Nikolaev Institute of Inorganic Chemistry SB RAS, 3, Acad. Lavrentiev Ave., Novosibirsk, 630090, Russia
E-mail: amikhailov@niic.nsc.ru
[b] Novosibirsk State University, 1, Pirogova str., Novosibirsk, 630090, Russia
[c] Prof. Dr. D. Schaniel and Dr. E. Wenger
Université de Lorraine, CNRS, CRM2, UMR 7036, Nancy, 54000, France

Abstract: The conditions for the photogeneration of NO linkage isomers at room temperature are studied. By pulsed laser irradiation in the blue spectral range the long-lived Ru-ON isomer can be generated at room temperature, which is crucial for potential applications such as holography and data storage. Using static and time-resolved spectroscopy (UV/Vis and IR) we give evidence that the liftime of the Ru-(η^2-(NO)) isomer is a decisive parameter for the formation of Ru-ON isomer at high temperature due to a two-step isomerization mechanism Ru-NO → Ru-(η^2-(NO)) → Ru-ON. Furthermore, we report the low temperature structures for each isomer, which were revealed by photocrystallography.

Introduction

Ruthenium nitrosyl coordination compounds are an interesting class of materials due to their ability to form photoinduced nitrosyl linkage isomers, an isonitrosyl Ru-ON (MS1) and a side-on Ru-(η^2-(NO)) (MS2) configuration,[1],[2] as well as their potential for photodynamic therapy.[3],[4] In order to be exploitable in applications, such as holography[5],[6] or data storage,[7] the underlying photoisomerization process needs to be understood in detail and should be producible at room temperature. In most cases, the generation and study of the linkage isomers is performed at low temperatures, where the MS1 and MS2 states exhibit an infinite lifetime.[8],[9],[10],[11] Room temperature studies were performed using transient absorption spectroscopy[12] and ultrafast pump-probe spectroscopy[13],[14],[15] on an iron nitrosyl compound (Sodium Nitroprusside, $Na_2[FeNO(CN)_5]2H_2O$). In the solid state, up to now, only the MS2 isomer could be observed at room temperature. This corroborates the hypothesis that for the generation of MS1 a two-step mechanism is necessary, whereby

MS1 is generated by inducing with a first photon MS2 and a second photon transfers MS2 to MS1.[16],[17],[18],[19],[20] In order to obtain MS1 one needs thus an overlap of GS and MS2 absorption bands in addition to the condition of a suitable relaxation path from the excited state to the linkage isomer energetic minimum (on the GS potential surface).[21] Actually, according to DFT[18] and MS-CASPT2[17] calculations the MS1 photogeneration pathway in $[RuCl(NO)(py)_4]^{2+}$ is supposed to involve several nonadiabatic intersystem crossing (ISC) processes between the singlet and triplet states of all three involved isomers GS, MS2, and MS1 (see e.g. Fig. 1 in Ref.[17]). In the current work we will not address these ISC processes, since they occur on time scales not accessible in our experiments. The reader should thus bear in mind that by the term „two-step mechanism“ we address a rather complicated multistep excitation-relaxation mechanism (for each step) of which we assess only the initial optical excitations as well as the thermal relaxation of GS, MS2 and MS1 within our experimental time resolution of a few nanoseconds.

In a recent work,[22] we have shown that the MS1 linkage isomer in $[RuNO(Py)_4F](ClO_4)_2$ can be generated by irradiation with 445 nm at low temperature (80 K) and that it exhibits the highest thermal stability of currently known NO linkage isomers. Furthermore, the MS2 linkage isomer can be generated by 980 nm irradiation of MS1. Given the rather long lifetime of MS1 (~10 min) at room temperature, this system is suitable to study the room temperature properties of NO linkage isomers. In the current work, we will thus discuss the generation mechanism of the linkage isomers in $[RuNO(Py)_4F](ClO_4)_2$ and especially explore the possibilities to generate the two linkage isomers at room temperature. For this purpose, we performed a systematic spectroscopic (UV/Vis and IR) study at low temperature and time-resolved

experiments at room temperature. Furthermore, we report the low temperature structures for MS1 and MS2 obtained from X-ray diffraction.

Results and Discussion

Photocrystallography investigations of GS, MS1 and MS2

In order to attribute spectroscopic features to the structural changes, the structures of all three isomers – GS, MS1 and MS2 of $[RuNO(Py)_4F](ClO_4)_2$ were determined by single crystal X-Ray diffraction at 100K (See Fig. 1). We describe here briefly the main structural changes in the Ru-NO group, for the complete discussion of the structures see the Supplementary Material (Fig. S1 and S2). The ground state (GS) structure contains two non – equivalent structural units with Ru1 and Ru2 central atoms. Ru-N distances (of Ru-NO) are 1.750 Å, Ru-N-O angles are close to linear: Ru1-N11-O111 = 177.5(1)°, Ru2-N21-O211 = 179.1(1)°. After 420 nm irradiation (60 min, 500mW), the color of the crystal changed from bright yellow to deep green (See Fig. S3), and the Ru-NO (GS) coordinate changes to Ru-ON (MS1) with 92 % population. The Ru-O bond distances in Ru-ON are 1.841 Å with 177.7(1) and 178.7(1)° Ru-O-N angles for Ru1 and Ru2 respectively. After subsequent 920 nm irradiation (30 min, 400 mW) of the same single crystal, the color changed from deep green to black (See Figure S3), and the structural parameters have been collected again. The MS2 isomer was found only for one structural unit with 17% population, with a Ru-N bond length of 2.00(2) Å and a Ru-O bond length of 2.09(1) Å. The Ru-N-O angle is 80(1)°. These photocrystallographic results allow us to unambiguously assign the spectral bands described in the sections below to the GS, MS1, and MS2 structures.

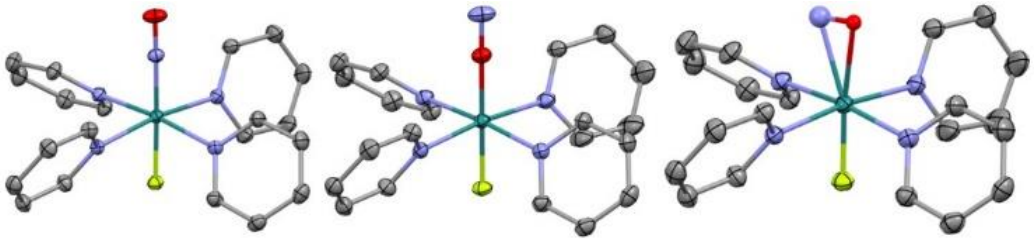

Figure 1. GS (Ru-NO, left), MS1 (Ru-ON, middle) and MS2 (Ru-(η^2-(NO)), right) structures in $[RuNO(Py)_4F](ClO_4)_2$ complex.

Low-temperature spectroscopy studies of linkage isomers

In order to find the optimal spectral range for photogeneration of MS1 and MS2 we performed a systematic infrared spectroscopic study using wavelengths in the range 365 - 1050 nm for population and depopulation of MS1 and MS2. Our results indicate that irradiation in the blue spectral range is the most efficient for transferring of GS to MS1 (Fig. 2). Under 405-470 nm exposure of GS, MS1 is generated as evidenced by two absorption bands with maxima at 1762 and 1768 cm^{-1}. Upon generation of MS1, the GS bands (two maxima at 1900 and 1912 cm^{-1}) decrease. Upon irradiation of MS1 using light in the 850 – 1050 nm spectral range, two simultaneous reactions occur – MS1 to GS and MS1 to MS2. The appearance of MS2 is reflected in the formation of bands with maxima at 1565 and 1580 cm^{-1}. The generation of MS2 is accompanied by a decreasing of MS1 and an increasing of GS bands. Population of both MS was determined from the decrease of the area of the GS band and amount to 40% for MS1 and 10 % for MS2. Irradiation with 365 and 505 – 780 nm light induces a bleaching of both MS1 and MS2 (See Fig. S7). The presence of two absorption bands for the nitrosyl stretching vibration band is due to two non-equivalent structural units in the unit cell. A summary of the wavelength dependence of the GS-MS transformations under light exposure is given in Figure S8.

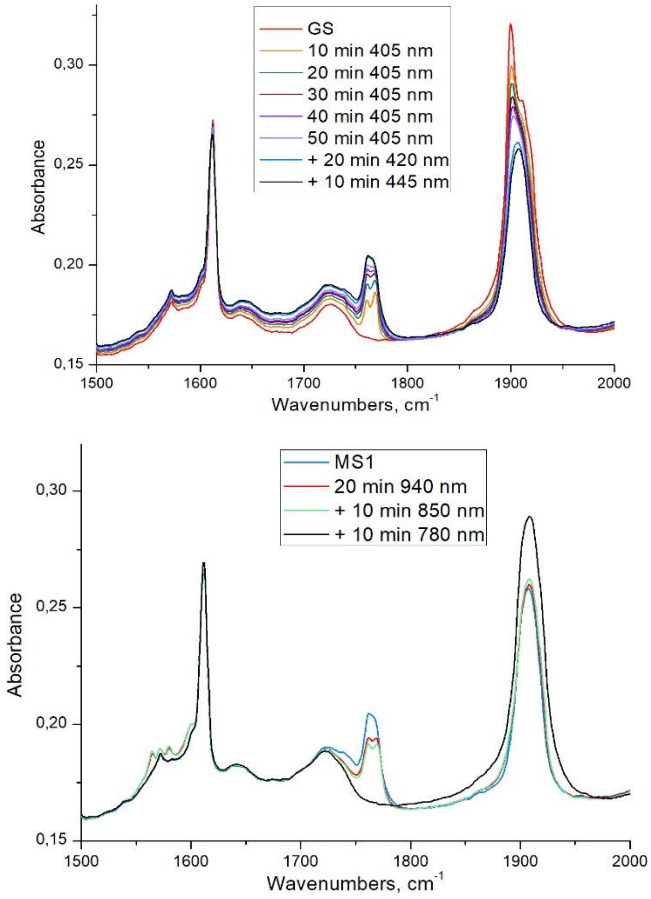

Figure 2. (Top) Decrease of GS bands (1900/1912 cm^{-1}) and increase of MS1 bands (1762/1768 cm^{-1}) as a function of exposure to blue light (405 - 445 nm) at 100 K (exposure time increases from red line = GS to black line). (Bottom) Decrease of MS1 bands (1762/1768 cm^{-1}) and increase of MS2 bands (1565/1580 cm^{-1}) and GS bands (1900/1912 cm^{-1}) as a function of irradiation in the near infrared spectral range: 940 nm (red line), 850 nm (green line), and 780 nm (black line).

In order to gain more insight into the population and depopulation processes of MS1 and MS2, the UV-vis spectra of the complex after light irradiation were measured at 100 K (See Fig. 3). The GS (red line) exhibits strong absorption from the deep UV up to the 500 nm region, while the MS1 (blue line) spectrum has another maximum around 660 nm. Concerning the MS2 (green line), it exhibits the strongest absorption with respect to GS and MS1 in the 500 - 600 nm region. Further irradiation of MS1 or MS2 by 780 nm light results in the spectrum marked in black, which is the same as the spectrum of GS except for an incomplete resumption of the band at ~400 nm. We attribute this difference to some nitric oxide release and the formation of the nitrosyl-deficient complex after long irradiation times (See Fig. S9). The UV-vis spectra give a first insight into the wavelength dependence of the MS1/MS2 population (See Fig. S8). GS can be transferred to MS1 by the 405 - 470 nm irradiation due to the strong absorption band at 405 - 470 nm region. As the absorbance of both MS1 and MS2 are shifted to the UV (365 nm) and the yellow – red (505 - 780 nm) spectral range with respect to GS, light irradiation in this region transfers MS1 and MS2 back to GS. Note that infrared light exposure (850 – 1050 nm) of MS1 opens the possibility to transfer MS1 to MS2. This indicates that the cross section for the transfer MS1-MS2 in this region is higher than that for MS2-GS (and/or MS1-GS).

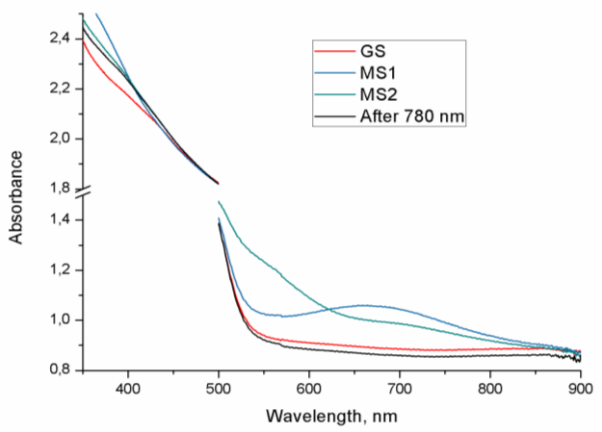

Figure 3. UV/vis spectra of GS at 100 K (red line, before irradiation), GS+MS1 (blue line, after 30 min of 445 nm), GS+MS1+MS2 (green line, after 100 min of 940 nm), and GS (black, after 30 min of 780 nm). The 350 - 500 nm range of the spectra was obtained from the $[RuNOPy_4F](ClO_4)_2$ complex in KBr pellet, the 500 – 900 nm range of the spectra from a $[RuNOPy_4F](ClO_4)_2$ single crystal.

The kinetic parameters of MS1 to GS and MS2 to GS reactions were determined by Differential Scanning Calorimetry (DSC) earlier[22]. Namely, the activation energy (E_a) and frequency factor (lgk_0) are 98.8 (4.3) kJ/mol and 14.9 (0.7), and 47.5 (4.2) kJ/mol and 10.4 (1.1) for MS1 – GS and MS2 – GS reactions respectively. According to this data, the lifetime (k^{-1} from the Arrhenius equation) of MS1 isomer at room temperature (293 K) is 9 min, which could provide the possibility to form the MS1 isomer at room temperature, not only at 80 – 100 K. However, irradiating during 10 min with 445 nm and 100 mW at room temperature does not yield a measureable MS1 signal in the infrared spectrum. In order to shine light on this behaviour we performed a temperature dependent study, where we repeated the same irradiation procedure (445nm, 10min, 100mW) at each temperature, before measuring the IR spectrum. We observe that the formation of MS1 under these conditions is only possible below temperatures of 230 K (Fig. 4.). The lifetime of MS1 at 230 K is $3.5 \cdot 10^7$ s, which indicates that it is not the lifetime of MS1 that prevents its detection (routine time of spectrum scan is 1 min). According to theoretical[18] as well as low-temperature absorption spectroscopy studies[16] of the nitrosyl isomerization mechanism in $[RuNOPy_4Cl]^{2+}$, the GS – MS1 reaction include the intermediate state MS2 and should be described as two step GS – MS2 – MS1 process. The lifetime of MS2 in $[RuNOPy_4F](ClO_4)_2$ at 230 K is 3 s (extrapolated from the DSC data). It seems thus probable that under the assumption of a GS – MS2 – MS1 mechanism of isomerization we encounter a temperature restriction of MS1 generation due to the small MS2 lifetime at high temperature, i.e. at high temperature (higher than 230 K) the probability of the second step, the MS2 – MS1 transformation, is very low, since the lifetime of MS2 is too small for «catching» of the second photon, especially in the case of a relatively low photon flux provided by an LED (445 mn, 100 mW). Indeed, if we compare our data with the data of other ruthenium complexes (See Table 1), there is a correlation between the maximum temperature at which MS1 can be populated and the lifetime of MS2 at this temperature. It seems that for different ruthenium complexes the lifetime of MS2 needs to be in the range of some seconds, in order to generate MS1 using irradiation with LED.

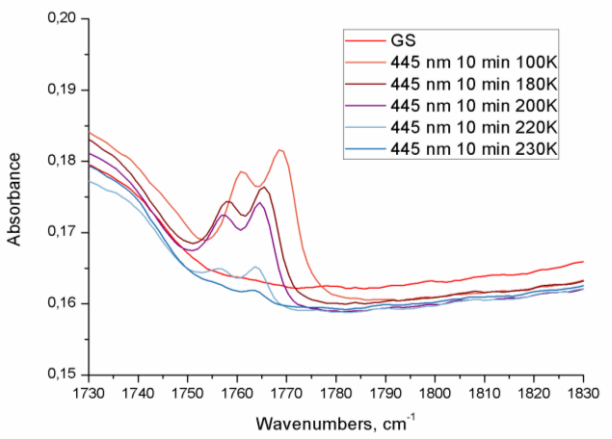

Figure 4. The generation of the MS1 isomer (445 nm, 10 min, 100 mW) at different temperatures: 100 K (orange line), 180 K (brown line), 200 K (purple line), 220 K (blue line), 230 K (dark blue line). The MS1 populations at these temperatures are 15, 8, 7, 3 and 1% respectively.

Table 1. Comparison of the maximum temperature T_{max} at which MS1 can be populated with the lifetime of MS2 at T_{max} for different ruthenium nitrosyl complexes.

Complex	T_{max}, K	MS2 lifetime, s	Ref.
$[RuNOPy_4Cl](PF_6)_2$	180	6	[23]
$[RuNO(NH_3)_4(H_2O)]Cl_3$	250	3	[9]
$[RuNO(NH_3)_5]Cl_3$	240	15	[9]
$[RuNOPy_4F](ClO_4)_2$	230	3	Pr. work

Generation of MS1 and MS2 at room temperature

Since the ratio between source power (watts or photons per second) and MS2 lifetime is crucial, we used a pulsed laser (10 Hz, 10 mJ, 445 nm, 5 ns) for generating MS1 at room temperature. The IR spectra of $[RuNOPy_4F](ClO_4)_2$ in KBr after 3 min of pulse laser irradiation at ≈300 K are shown in Fig. 5. The position of the newly generated bands is the same (1755 and 1761 cm^{-1}) as in the low temperature experiment after blue light exposure, the slight shift to lower energy of 7 cm^{-1} is expected due to the higher temperature. These generated bands decay with a lifetime of 151 s, which corresponds to the calculated MS1 lifetime at 302 K. Hence, according to the position and decay time of the band, we assign the band to the MS1 NO stretching vibration. There were no measurable changes in the IR spectrum in the case of less than 1 min of pulsed irradiation with 445 nm as well as in the case of pulsed irradiation with 590 nm for 3 min. The fact that MS1 can be photogenerated at room temperature using pulse light source is in agreement with the proposed two-step generation mechanism GS - MS2 – MS1. The higher photon flux per unit time provided by the short pulse increases the probability to induce the second step MS2-MS1. To the best of our knowledge, this is the first example of MS1 formation at room temperature in the solid state for ruthenium nitrosyl complexes.

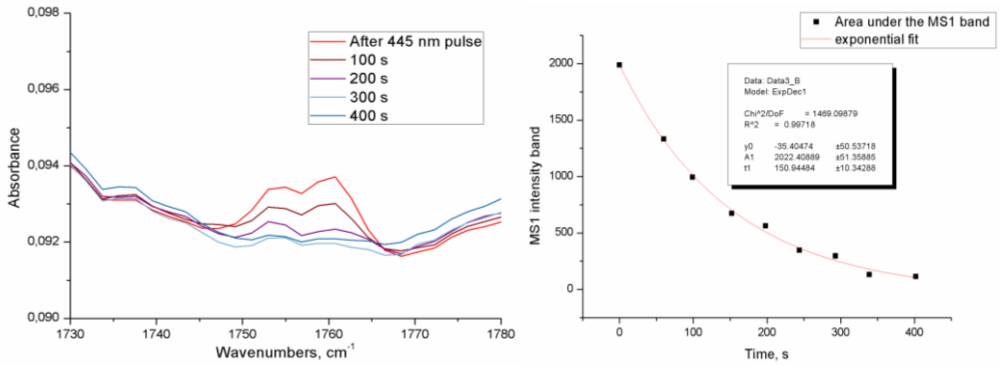

Figure 5. (Top) IR spectra of $[RuNOPy_4F](ClO_4)_2$ in KBr after 3 min of pulse laser irradiation at ≈300 K as a function of time. (Bottom) Mono-exponential fit of the band area during the decay. The lifetime of the band is 151 s at ≈300 K, the band's decay is assigned to the MS1 thermal decay process.

In order to further support the proposed isomerization mechanism (GS - MS2 – MS1), the light – induced absorption at room temperature has been measured using transient pump – probe spectroscopy. Temporal decay of the light-induced absorption after pumping with a 445 nm laser pulse in a $[RuNOPy_4F](ClO_4)_2$ single crystal is shown in Fig. 6 and Fig. S10. The absorption decay is fitted by mono-exponential kinetic and characterized by a 8.5 - 18 ms lifetime, for different probe wavelengths. According to DSC data, the lifetime of the MS2 isomer at 300 K is 7.5 ms, which suggests, that the detected light-induced absorption change corresponds to the MS2 state and its thermal decay process. All findings show, that after excitation of $[RuNOPy_4F](ClO_4)_2$ with a single laser pulse a significant amount of the MS2 state can be populated, while the MS1 population is too small to be detected in our experiment. Long-time irradiation with a pulsed laser (3 minutes with 10Hz repetition rate corresponding to 1800 pulses) allows to generate a measurable amount of MS1 state by a sequential two-step photon absorption from GS to MS2 to MS1. Note that the generation of MS1 occurs within one single laser pulse, since the MS2 state relaxes faster than 100 ms, the delay between two laser pulses in our experiment. From literature we know that the photoisomerization from GS to MS2 is complete within a few picoseconds[13],[14], so that there remains enough time in the MS2 state to absorb a second photon of the 5 ns long impinging laser pulse. However, based on the methods used in this work we cannot decipher the details of the complicated isomerization mechanism via non-adiabatic processes and interplay between singlet and triplet channels proposed by theory[17],[18] . Notwithstanding, our results are unambiguous experimental evidence for the two-step mechanism (GS-MS2-MS1) of nitrosyl ligand photoisomerization within the meaning that two photons are needed to drive the system from GS to MS1 (via MS2). Most importantly, our results show that, given the appropriate wavelength and photon flux, MS1 can be generated at room temperature.

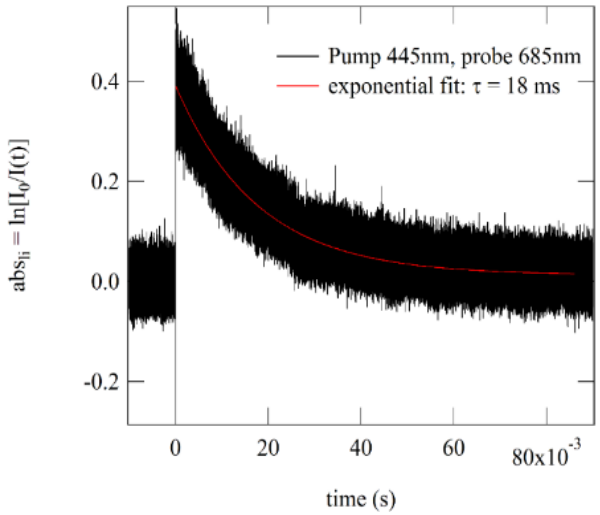

Figure 6. Light-induced absorption changes in $[RuNOPy_4F](ClO_4)_2$ single crystal after pumping at 445 nm (5 ns laser pulse) and probing at 685 nm. The experimental data is fitted by mono-exponential kinetic yielding a lifetime of 18 ms.

Conclusions

The described results for the generation of nitrosyl linkage isomers at room temperature open new avenues for the activation of small molecules by light. As was shown, due to the two-stage isomerization mechanism GS-MS2-MS1, the short life-time intermediate MS2 could restrict the formation of the long-lived MS1 isomer. This main drawback for room temperature applications can be overcome by using a sufficiently high photon flux as given, e.g., by a pulsed laser source. Since each linkage isomer has particular absorption properties, the proper choice of the photoexcitation wavelength will allow to drive the isomerization route.

Experimental Section

Synthesis of *trans*-$[RuNO(Py)_4F](ClO_4)_2$

Synthesis of $[RuNO(Py)_4F](ClO_4)_2$ was performed as described in previous work.[22] Short description is given: 347 mg of $[RuNO(Py)_4OH](PF_6)_2$ was dissolved in 10 mL of HF and heated in a closed polypropylene vessel for 6 h at 85 °C. The solution then was evaporated in air to a minimum volume and 6 mL of 6 M $HClO_4$ was added. The yellow powder of $[RuNO(Py)_4F](ClO_4)_2$ complex was precipitated by diethyl ether, filtered and washed with diethyl ether. The yield of $[RuNO(Py)_4F](ClO_4)_2$ is 72%. The single crystals of $[RuNO(Py)_4F](ClO_4)_2$ used for all measurements were obtained by recrystallization from water.

Infrared and UV/vis spectroscopy

Infrared spectroscopy measurements with irradiation were performed using a Nicolet 5700 FT-IR spectrometer with a resolution of 2 cm^{-1} in the range 400 − 4000 cm^{-1}. The sample was grinded, mixed with KBr, and pressed into pellets. KBr pellets were bonded by silver paste on the coldfinger of a closed cycle cryostat (Oxford Optistat V01) and irradiated by LED through KBr windows with light of different wavelengths in the range 365−1050 nm and 15-150 mW optical power. The cryostat allows controlling the temperature in the range of 9−320 K. UV/vis spectra were recorded using transparent KBr pellets or single crystals of the complex with a Varian CARY 4000 spectrometer. Transparent pellets were prepared as for IR measurements. Low-temperature measurements were performed using the same cryostat as for IR measurements, except that KBr windows were exchanged for standard borosilicate glass windows. For single-crystal measurements, the single crystals were mounted on a diaphragm, in order to block all parts of the probe beam not passing through the sample. The baseline was measured using the same diaphragm, which can be mounted on the cryostat sample holder.

Pump-Probe Transient Absorption Spectroscopy

The optical pump system consists of a Surelite II-10 Nd-YAG pulsed laser equipped with an optical parametric oscillator (OPO, model SLOPO+). The system delivers laser pulses with 3-5 ns duration at a frequency of 10 Hz. The OPO is tunable in the range 400-700 nm. The laser beam is directed to the sample position (single crystal or KBr pellet) using a series of silver-coated mirrors and precisely adjusted and focused through appropriate lenses (f=100, 200, or 300) to illuminate the sample uniformly (i.e. the beam diameter is larger than the sample). For the transient absorption measurements cw-LASERs at different wavelengths (532 nm, 635 nm and 685 nm) are used to probe the light-induced absorption. The probe beam is focused by a lens (f=300) on the sample position such that the probe beam diameter is smaller than the pump beam diameter. Its intensity can be adjusted by a λ/2 waveplate and a polarizer from a few mW to a few µW. The probe light is detected by a 200MHz Si-Pin diode from Femto Messtechnik GmbH. The voltage at the output of the detector is sampled using a 1.5-GHz oscilloscope (Lecroy Wavepro 715zi). The trigger is obtained directly from the LASER control system (delay of 10 ns with respect to the arrival of the pump beam on the sample position). In order to block the pump light (445 nm) appropriate color filters (OG515 or OG590) and interference filters at the corresponding probe wavelengths (width of 5 nm) are mounted in front of the photodiode. The system allows either single-shot excitation or repetitive excitation with 10 Hz. In the single-shot mode the pump pulse is triggered by manual control and the delay time between two pulses and the recording time can be adjusted at will. The transient absorption signal is recorded in single-shot mode and averaged over 20 pump-probe cycles. For the infrared spectroscopic experiments the KBr pellets of $[RuNO(Py)_4F](ClO_4)_2$ are excited in the 10 Hz mode, i.e. the delay between two pump pulses is 100 ms. The exposure time is monitored by a chronometer to 1 min or 3 min, corresponding to 600 and 1800 pulses respectively. The pulse intensity (measured over the beam size of 13 mm diameter covering the KBr pellet size) is 100 mW (corresponding to 10 mJ/pulse) at 445nm.

Single crystal X-ray diffraction

One unique single crystal of $[RuNO(Py)_4F](ClO_4)_2$ was selected and measured with a D8 Venture Bruker 4 circles diffractometer. This diffractometer is equipped with an Incoatec IµS microfocus X-ray source with a Molybdenum anode (MoKα, λ = 0.71073 Å) and a PHOTON II detector. An Oxford Cryosystems Cryostream nitrogen blower was used to fix the sample temperature. Using Olex2,[24] structures were solved with the XS[25] structure solution program using Direct Methods and refined with the XL[25] refinement package using Least Squares minimization. For irradiation procedures 420 nm 500 mW and 920 nm 400 mW LED were used for generating of MS1 and MS2 respectively. All X-Ray experiments were carried on the same single crystal. Structures have been deposited in CCDC with code numbers 1900341, 1900344, 1900342, 1900343 for GS, MS1, MS2 and GS after relaxation respectively.

Acknowledgements

This work was supported by the Comprehensive Program of Fundamental Research (Project 19-03-00594 A). Also, we thank Federal Agency for Scientific Organizations for funding. Artem Mikhailov is grateful for financial support from the Eiffel excellence bourse program (Grant P730329G).

References

[1] P. Coppens, I. Novozhilova, A. Kovalevsky, *Chem. Rev.* **2002**, *102*, 861–884.

[2] D. V. Fomitchev, P. Coppens, *Inorg. Chem.* **1996**, *35*, 7021–7026.

[3] R. R. Allison, C. Sheng, R. Cuenca, V. S. Bagnato, C. Austerlitz, C. H. Sibata, *Photodiagnosis Photodyn. Ther.* **2010**, *7*, 115–119.

[4] A. A. Mikhailov, V. A. Vorobyev, V. A. Nadolinny, Y. V. Patrushev, Y. S. Yudina, G. A. Kostin, *J. Photochem. Photobiol. A Chem.* **2019**, *373*, 37–44.

[5] D. Schaniel, M. Imlau, T. Weisemoeller, T. Woike, K. W. Krämer, H.-U. Güdel, *Adv. Mater.* **2007**, *19*, 723–726.

[6] M. Goulkov, D. Schaniel, T. Woike, *J. Opt. Soc. Am. B* **2010**, *27*, 927.

[7] T. Woike, W. Kirchner, G. Schetter, T. Barthel, K. Hyung-sang, S. Haussühl, *Opt. Commun.* **1994**, *106*, 6–10.

[8] B. Cormary, I. Malfant, M. Buron-Le Cointe, L. Toupet, B. Delley, D. Schaniel, N. Mockus, T. Woike, K. Fejfarová, V. Petříček, et al., *Acta Crystallogr. Sect. B Struct. Sci.* **2009**, *65*, 612–623.

[9] D. Schaniel, T. Woike, B. Delley, C. Boskovic, D. Biner, K. W. Krämer, H. U. Güdel, *Phys. Chem. Chem. Phys.* **2005**, *7*, 1164–1170.

[10] G. A. Kostin, A. O. Borodin, A. A. Mikhailov, N. V. Kuratieva, B. A. Kolesov, D. P. Pishchur, T. Woike, D. Schaniel, *Eur. J. Inorg. Chem.* **2015**, *29*, 4905–4913.

[11] G. A. Kostin, A. A. Mikhailov, N. V. Kuratieva, D. P. Pischur, D. O. Zharkov, I. R. Grin, *New J. Chem.* **2017**, *41*, 7758–7765.

[12] D. Schaniel, T. Woike, C. Merschjann, M. Imlau, *Phys. Rev. B* **2005**, *72*, 195119.

[13] D. Schaniel, M. Nicoul, T. Woike, *Phys. Chem. Chem. Phys.* **2010**, *12*, 9029–9033.

[14] G. Gallé, M. Nicoul, T. Woike, D. Schaniel, E. Freysz, *Chem. Phys. Lett.* **2012**, *552*, 64–68.

[15] M. S. Lynch, M. Cheng, B. E. Van Kuiken, M. Khalil, *J. Am. Chem. Soc.* **2011**, *133*, 5255–5262.

[16] L. Khadeeva, W. Kaszub, M. Lorenc, I. Malfant, M. Buron-Le Cointe, *Inorg. Chem.* **2016**, *55*, 4117–4123.

[17] F. Talotta, J.-L. Heully, F. Alary, I. M. Dixon, L. González, M. Boggio-Pasqua, *J. Chem. Theory Comput.* **2017**, *13*, 6120–6130.

[18] J. Sanz García, F. Alary, M. Boggio-Pasqua, I. M. Dixon, I. Malfant, J.-L. Heully, *Inorg. Chem.* **2015**, *54*, 8310–8318.

[19] D. Schaniel, T. Woike, C. Boskovic, H. U. Güdel, *Chem. Phys. Lett.* **2004**, *390*, 347–351.

[20] S. I. Gorelsky, A. B. P. Lever, *Int. J. Quantum Chem.* **2000**, *80*, 636–645.

[21] D. Schaniel, T. Woike, *Phys. Chem. Chem. Phys.* **2009**, *11*, 4391–4395.

[22] G. A. Kostin, A. A. Mikhailov, N. V Kuratieva, D. P. Pishchur, A. N. Makhinya, *New J. Chem.* **2018**, *42*, 18928–18934.

[23] D. Schaniel, B. Cormary, I. Malfant, L. Valade, T. Woike, B. Delley, K. W. Krämer, H. U. Güdel, *Phys. Chem. Chem. Phys.* **2007**, *9*, 3717–3724.

[24] O. V. Dolomanov, L. J. Bourhis, R. J. Gildea, J. A. K. Howard, H. Puschmann, *J. Appl. Crystallogr.* **2009**, *42*, 339–341.

[25] G. M. Sheldrick, *Acta Crystallogr. Sect. A Found. Crystallogr.* **2008**, *64*, 112–122.

Supplementary materials

Structures of GS, MS1 and MS2

GS structure refinement

The GS structure of the complex is comparable to the one from previous work[1]. The unit cell contains two non – equivalent structural units with Ru1 and Ru2 central atoms (See Figures S1 and S2). The cell parameters are given in Table S1. Ru-N bond distances in the Ru-NO groups are 1.751(1) and 1.750(1) Å for Ru1 and Ru2 respectively (See Table S2). The N-O distances of the NO groups are equal: N-O = 1.141(2) Å. The Ru-N-O angles are close to linear: Ru1-N11-O111 = 177.5(1)°, Ru2-N21-O211 = 179.1(1)°. The average distances between Ru and planar N atoms of pyridine ligands are 2.092(2) and 2.098(2) Å for Ru1 and Ru2, respectively. The average angles between N donor pyridine atom, ruthenium and N11(N21) atom of nitrosyl ligand are 93.5(5) and 94.0(4)° for Ru1 and Ru2, respectively (See Table S1). Pyridine rings demonstrate a propeller like type, as found for the $[RuNOPy_4Cl](PF_6)_2$ complex[2]. Ru-F distances show significant differences: Ru1-F1 = 1.960(1) Å and Ru2-F2 = 1.914(1) Å, which could be attributed to the packing features of each structural unit. The nitrosyl groups are each surrounded by three perchlorates anions. The corresponding O-O closest distances are O111-O43 = 2.760(3) Å, O111-O34 = 2.887(2) Å, O111-O11 = 2.986(2) Å for Ru1 and O211-O41 = 2.796(2) Å, O211-O31 = 2.836(3) Å, O211-O21 = 3.129(2) Å for Ru2.

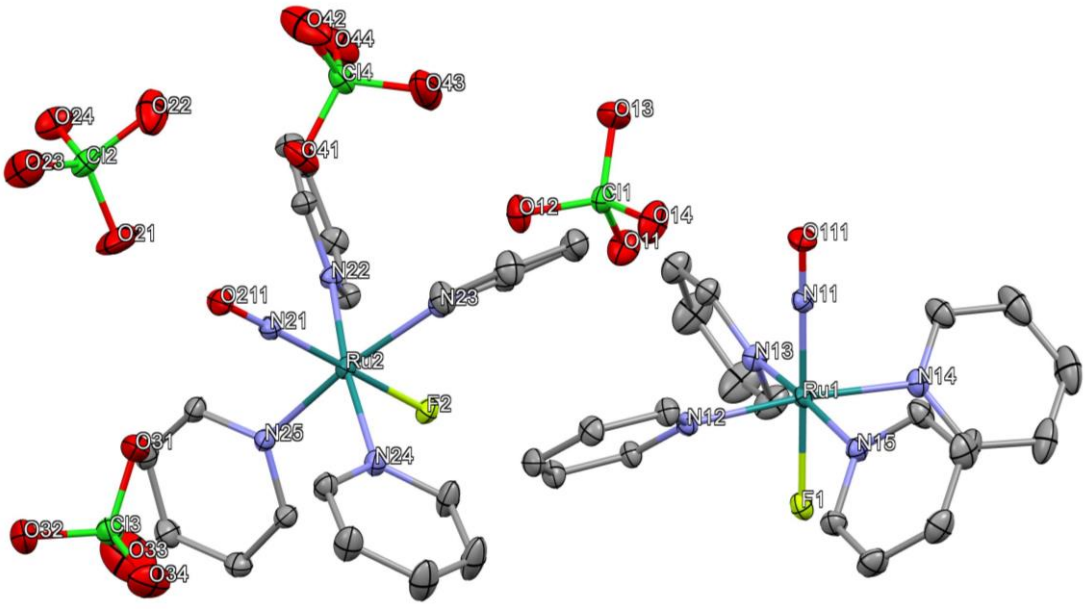

Figure S1. GS structure of $[RuNOPy_4F](ClO_4)_2$ complex. Hydrogen atoms are omitted.

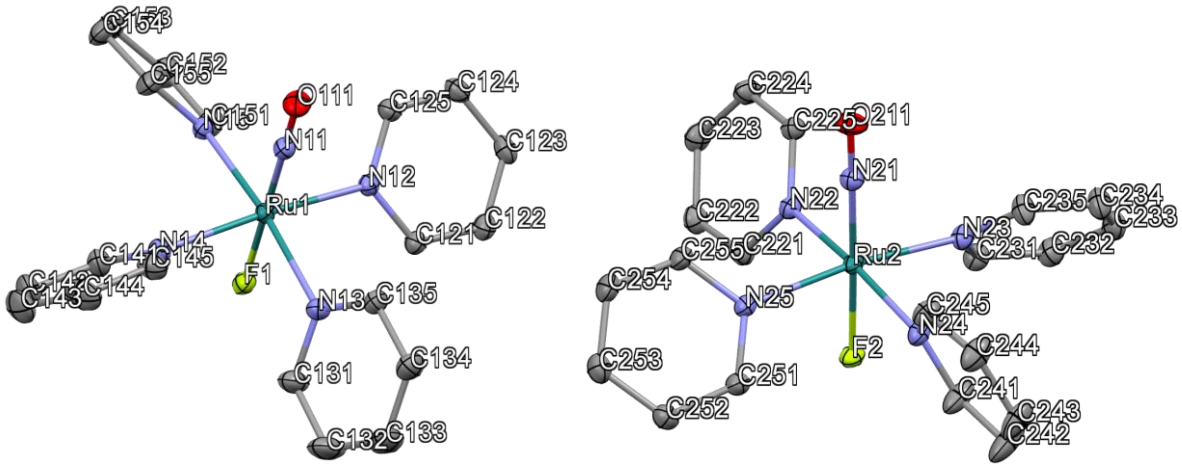

Figure S2. GS structure of $[RuNOPy_4F](ClO_4)_2$ complex. Ru1 complex is placed on the right, Ru2 – on the left. Anions (ClO_4^-) and hydrogen atoms are omitted.

Table S1. Experimental and refinement details. *R* factor of MS1 is shown for refinement only with Ru-ON isomer, *R* factor of MS2 – for model with partial occupation of GS, MS1 and MS2.

	GS	MS1	MS2	GS after
Formula	$C_{20}H_{20}N_5O_9F_1Cl_2Ru$			
Formula weight	665.38			
Temperature/K	100			293
Crystal system	Triclinic			
Space group	$P\bar{1}$			
a/Å	10.426(1)	10.494(1)	10.438(1)	10.5287(9)
b/Å	16.431(2)	16.349(2)	16.407(2)	16.640(2)
c/Å	16.397(2)	16.368(2)	16.413(2)	16.699(2)
α/°	65.866(4)	65.582(3)	65.912(4)	65.407(3)
β/°	82.813(4)	82.680(3)	82.720(4)	82.816(3)
γ/°	87.451(4)	88.181(3)	87.832(4)	87.979(3)
Volume/Å^3	2543.2(5)	2535.4(4)	2544.9(5)	2638.9(4)
Z/Z’	2/2			
ρ_{calc}g/cm^3	1.738	1.743	1.737	1.675
μ/mm^{-1}	0.893	0.896	0.893	0.861
F(000)	1336.0			
Crystal size/mm^3	0.228 × 0.213 × 0.192			
Radiation	MoKα (λ = 0.71073)			

2Θ range for data collection/°	2.716 to 76.118	2.736 to 71.646	2.72 to 72.556	2.692 to 61.274
Index ranges	-18 ≤ h ≤ 18, -28 ≤ k ≤ 28, -27 ≤ l ≤ 27	-17 ≤ h ≤ 17, -26 ≤ k ≤ 26, -26 ≤ l ≤ 26	-17 ≤ h ≤ 17, -27 ≤ k ≤ 27, -27 ≤ l ≤ 27	15 ≤ h ≤ 14, -23 ≤ k ≤ 23, -23 ≤ l ≤ 23
Reflections collected	163780	200391	170726	122480
Independent reflections	26806 [R_{int} = 0.0462, R_{sigma} = 0.0321]	23648 [R_{int} = 0.0491, R_{sigma} = 0.0254]	24469 [R_{int} = 0.0583, R_{sigma} = 0.0347]	16105 [R_{int} = 0.0327, R_{sigma} = 0.0205]
Data/restraints/parameters	26806/0/686	23648/0/733	24469/0/751	16105/0/685
Goodness-of-fit on F^2	1.051	1.085	1.046	1.045
Final R indexes [I>=2σ (I)]	R_1 = 0.0333, wR_2 = 0.0755	R_1 = 0.0346, wR_2 = 0.0784	R_1 = 0.0400, wR_2 = 0.0944	R_1 = 0.0431, wR_2 = 0.1210
Final R indexes [all data]	R_1 = 0.0463, wR_2 = 0.0847	R_1 = 0.0469, wR_2 = 0.0872	R_1 = 0.0536, wR_2 = 0.1045	R_1 = 0.0621, wR_2 = 0.1407
Largest diff. peak/hole / e $Å^{-3}$	1.82/-1.63	1.81/-1.04	1.51/-1.31	1.03/-0.73

Table S2. Selected bond distances and angles of GS, MS1 and MS2 isomers.

Distance/angle [Å/°]	GS	MS1	MS2 (GS for Ru1)	$GS_{after\ relaxation}$
Ru1-N11	1.751(1)	-	1.800(7)	1.760(2)
Ru1-O111	-	1.842(1)	-	-
N11-O111	1.141(2)	1.146(2)	1.10(1)	1.127(4)
Ru1-N11-O111	177.5(1)	-	176.4(8)	177.7(3)
Ru1-O111-N11	-	177.7(1)	-	-
Ru1-F1	1.960(1)	1.943(1)	1.952(1)	1.954(2)
Ru1-N12	2.097(2)	2.096(2)	2.094(2)	2.104(3)
Ru1-N13	2.090(1)	2.085(1)	2.086(1)	2.091(2)
Ru1-N14	2.087(2)	2.085(2)	2.086(2)	2.096(3)
Ru1-N15	2.094(1)	2.085(1)	2.087(1)	2.097(2)
Ru2-N21	1.750(1)	-	2.00(2)	1.757(3)

Ru2-O211	-	1.841(1)	2.09(1)	-
N21-O211	1.141(2)	1.146(2)	1.03(2)	1.135(5)
Ru2-N21-O211	179.1(1)	-	80(1)	178.7(3)
Ru2-O211-N21	-	178.7(1)	71(1)	-
Ru2-F2	1.914(1)	1.898(1)	1.907(1)	1.908(2)
Ru2-N22	2.098(1)	2.091(1)	2.092(1)	2.098(2)
Ru2-N23	2.098(2)	2.091(2)	2.092(2)	2.096(3)
Ru2-N24	2.103(2)	2.095(1)	2.100(2)	2.099(3)
Ru2-N25	2.092(1)	2.086(2)	2.089(2)	2.098(3)

Table S3. Selected angles and torsion angles in $[RuNOPy_4F](ClO_4)_2$ complex.

Angle [°]	GS	MS1 (O111 and O211 instead of N11 and N21)	MS2 (N212 instead of N21)	GS after
N12-Ru1-N11	92.83(6)	91.46(6)	92.1(2)	93.1(1)
N13-Ru1-N11	94.64(6)	93.13(7)	94.1(2)	94.1(1)
N14-Ru1-N11	93.81(6)	92.76(6)	93.6(2)	93.5(1)
N15-Ru1-N11	92.60(6)	92.32(6)	92.6(2)	92.4(1)
F1-Ru1-N11	177.97(5)	178.38(5)	178.0(2)	178.5(1)
C121-N12-Ru1-N11	131.3(1)	131.1(1)	131.0(3)	131.3(2)
C131-N13-Ru1-N11	154.0(1)	154.1(2)	152.9(4)	151.2(3)
C141-N14-Ru1-N11	140.2(1)	141.1(1)	140.8(3)	140.9(3)
C151-N15-Ru1-N11	141.0(1)	141.8(1)	141.9(4)	142.6(3)
N22-Ru2-N21	93.34(6)	93.10(6)	93.04(9)	93.6(1)
N23-Ru2-N21	94.64(6)	93.48(6)	94.42(9)	93.9(1)
N24-Ru2-N21	94.64(6)	92.75(6)	94.12(9)	93.6(1)
N25-Ru2-N21	93.29(6)	92.50(6)	93.53(9)	93.3(1)
F2-Ru2-N21	178.78(5)	179.30(5)	178.82(9)	179.3(1)
C221-N22-Ru2-N21	149.3(1)	149.4(1)	149.0(2)	150.0(3)
C231-N23-Ru2-N21	146.2(1)	149.2(1)	146.8(2)	147.8(3)
C241-N24-Ru2-N21	159.3(1)	145.6(2)	159.0(2)	157.2(3)
C251-N25-Ru2-N21	137.4(1)	136.9(1)	136.8(2)	138.3(3)

MS1 structure refinement

After irradiation of the same single crystal with blue light (420 nm, 60min, 500 mW), the color of the crystal changed from bright yellow to deep green (See Figure S3) and the structural parameters have been collected again. Lattice parameters changed as well, as illustrated in Table S1. The *a* constant, which mainly corresponds to the axis along the ruthenium-nitrosyl coordinate elongated from 10.426(1) to 10.494(1) Å (0.6%), while *b* and *c* constants decreased from 16.431(2) and 16.397(2) Å to 16.349(2) (0.5%) and 16.368(2) Å (0.2%), respectively. For the determination of the atomic position we apply an approach that was used earlier[3],[4]. The structure was solved with three different models: *a* – with Ru-NO bonds; *b* – with Ru-ON bonds; *c* – with both Ru-NO and Ru-ON linkage types. Then, the residual electron density maps for each type of refinement were drawn and analyzed (See Figure S4). The map obtained using model *a* shows significant excess of electrons around the nitrogen atom and a corresponding depletion of electron density around the oxygen atom of the nitrosyl ligand, which indicates that a more electron rich atom should be placed at the GS nitrogen position and a less electron rich atom at the GS oxygen position. In the case of a structure refinement with Ru-ON groups (Figure S4, model *b*), no significant excess or depletion of electron density around the isonitrosyl ligands is observed, indicating that the occupation of this type of isomers is close to full. Finally, the disordered structure with both a Ru-NO and a Ru-ON configuration (model *c*) does not demonstrate any depletion or excess of electron density around iso- and nitrosyl ligands either. In this case, the occupancies of Ru1-O111-N11 and Ru2-O211-N21 groups are 95 and 89%, corresponding to an almost full GS – MS1 conversion. Unfortunately, Ru-NO of the remaining 5 and 11% GS could not be refined with anisotropic displacement parameters due to the low occupancy. For an in-depth discussion of the correlation between population and structural and anisotropic displacement parameters we refer the reader to the work by Cormary et al.[2]. As the populations of MS1 are almost 100%, we give only the parameters obtained from model *b* in the Tables S1, S2 and S3. The Ru-O bond distances in Ru-ON are 1.842(1) and 1.841(1) Å for Ru1 and Ru2 respectively. Clearly, in MS1 Ru-ON bond distances are longer by 0.091(1) Å compared to GS, and this is the most drastic change in bond distances after light exposure. N-O distances are slightly elongated – 1.146(2) Å. Ru1-O111-N11 and Ru2-O211-N21 angles are still close to linear – 177.7(1) and 178.7(1)°. Ru-F distances decreased by 0.017(1) and 0.016(1) Å compared to GS to Ru1-F1 = 1.943(1) Å and Ru2-F2 = 1.898(1) Å. The average distances between Ru and planar N atoms of pyridine are 2.088(3) and 2.091(2) Å for Ru1 and Ru2 respectively, which decreased by 0.004(3) and 0.007(2) Å, compared to GS. The average angles between N pyridine atom, ruthenium and O111 (O211) atom of isonitrosyl ligand are 92.4(4) and 93.0(2)° for Ru1 and Ru2 respectively, corresponding to an upward tilting of the pyridine rings by 1.1(5) and 1.0(4) °. Pyridine torsions are changed as well after NO isomerization. One of the pyridine ring propeller change the

orientation drastically by 13.7(2)° (See Table S3). While the displacement parameters of pyridine rings remain the same before and after isomerization, the significantly increased displacement parameters of the perchlorate oxygen atoms indicate a disorder over two positions of the perchlorate counter ions after isomerization. The N-O closest distances between nitrosyl and perchlorate for Ru1 are: N11-O43 – 2.725(4) Å, N11-O34 - 2.903(3) Å, N11-O11 – 2.932(3) Å; for Ru2: N21-O41 – 2.777(3) Å, N21-O31 – 2.841(3) Å, N21-O21 – 2.74(4) Å. Probably, the interaction between the nitrosyl group and the perchlorate changes after isomerization and thus affects the disordering of oxygen positions, which results in an increase of the thermal displacement parameters. In general, changing of the linkage from Ru-NO to Ru-ON affects all bond distances and angles in the ruthenium octahedron and the second coordination sphere. With elongation of the Ru-ON coordinate, the structure adapts to the new linkage – thereby affecting the other distances and angles in the first coordination sphere. Our structural refinement indicates an MS1 isomer with almost 100% population, while from IR data, the population of MS1 was only 40%. This difference might be due to the different nature of the sample (powder in KBr pellet vs single crystal). Note that this is one of the three example[2],[3] with the highest MS1 population, which shows how the whole structure changes after a rather small rearrangement of one ligand.

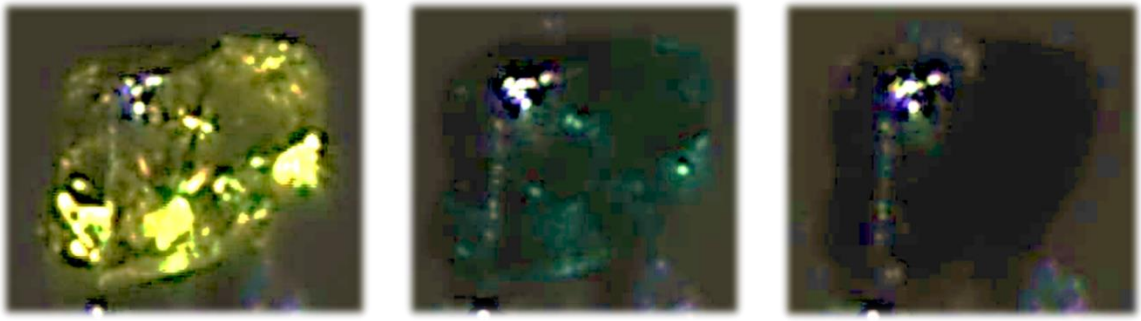

Figure S3. The color of single crystal of $[RuNOPy_4F](ClO_4)_2$ complex in GS (left, yellow), MS1 (middle, deep green) and MS2 (right, black).

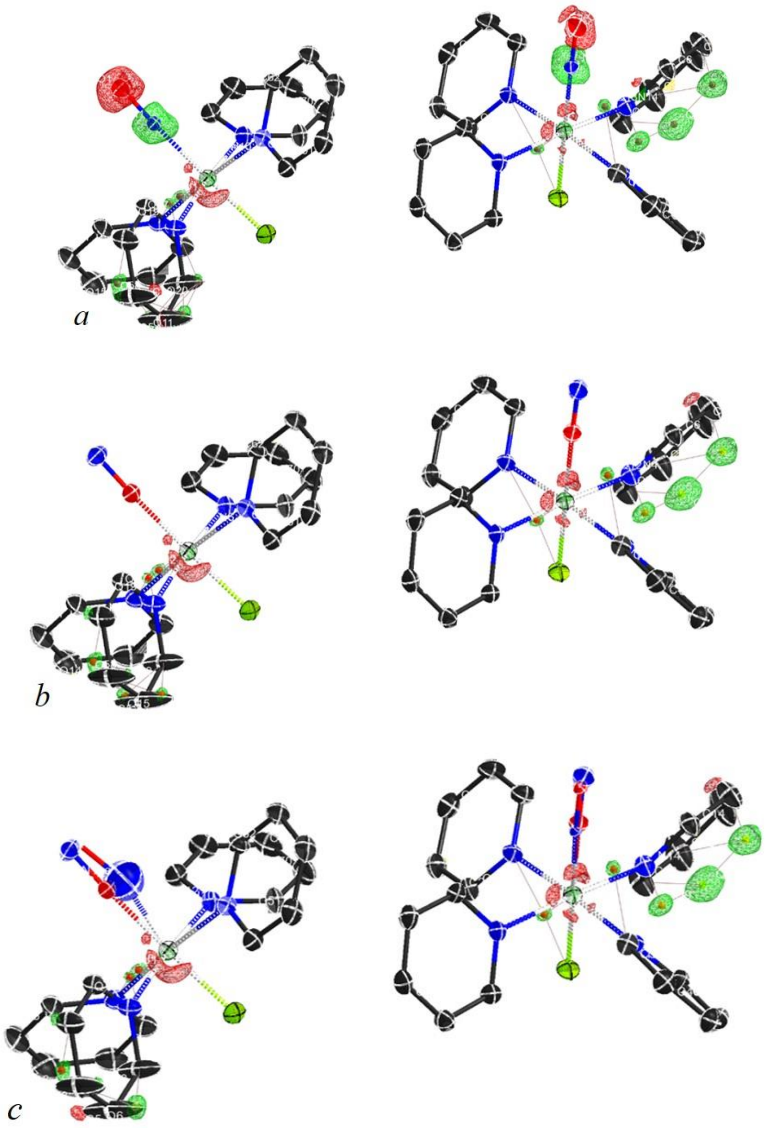

Figure S4. Residual electron density maps of structure refinement with Ru-NO (*a*, top), Ru-ON (*b*, middle) groups and both groups (*c*, bottom). Occupancies of Ru-NO isomers in the last model are 5 and 11% for Ru1 and Ru2 respectively. Ru1 fragment is placed on the left, Ru2 – on the right. Excess of electrons is shown by the green color, depletion by the red color. The residual electron density surfaces are 0.4 eÅ^{-3}.

MS2 structure refinement

After subsequent irradiation of the same single crystal with infrared light (920 nm, 30 min, 400 mW) the color of the crystal changed from deep green to black (See Figure S3), and the structural parameters have been collected again. The cell parameters changed with a trend back towards those of GS – *a* decreased, *b* and *c* increased. The structure was solved and refined using different models as discussed below. During the refinement, an electronic density corresponding to the MS2 isomer was detected only in the Ru2 fragment. Residual electron density maps of the different refinement models are shown in Figure S5. Interestingly we observe an MS2 population only for the Ru2 complex. The reason for this difference is at

the moment not clear, we can only speculate about possible origins. We know that the ligand trans to nitrosyl has a strong influence on the photoisomerization[5], we therefore suppose that the difference in Ru-F bond lengths of the two non-equivalent Ru1 and Ru2 complexes is responsible for the different MS2 populations. In the case of a structure refinement assuming a Ru-NO group (See Figure S5, *a*), we can clearly distinguish an excess of electrons in the perpendicular plane near the nitrosyl group in Ru2. Moreover, there is depletion of electrons near the oxygen atom of the nitrosyl ligand. Both observations shows us, that all three possible states – GS, MS1 and MS2 are present in Ru2, i.e. the transfer from MS1 to MS2 is not complete. According to Ru-ON refinement (Figure S8, *b*), excess of electrons in the perpendicular plane of nitrosyl of Ru2 shows up again as well as depletion of electrons near the oxygen atom of the nitrosyl ligand. In the last model, we laid two Ru-NO and Ru-(η^2-(NO)) groups in the Ru2 structure (Figure S8, *c*). This refinement does not demonstrate any lack or excess of electrons around the nitrosyl ligands. Even with only 17% occupancy of MS2 isomer, we can unambiguously refine the MS2 structure, as it is located perpendicular to the GS or MS1 coordinate. However, due to the low occupancy, we could not manage to refine Ru-(η^2-(NO)) with anisotropic displacement parameters. As was mentioned above, in this system all three possible linkage states are present, thus, we limit our discussion to the changes related to the nitrosyl ligand of MS2. The structure of MS2 is presented in Figure S6. Ru2-N21 bond length is 2.00(2) Å, Ru2-O211 bond is longer – 2.09(1) Å, which is in agreement with MS2 structural data of the $[RuNOPy_4Cl](PF_6)_2$ complex – 1.92(1) and 2.14(1) Å. N21-O211 distance is 1.03(2) Å. The Ru2-N21-O211 angle is 80(1)°, which is close to 90°, Ru2-O211-N21 = 71(1)°. Ru2-N212 bond of the remaining GS component is 1.765(2) Å, N212-O212 = 1.152(3) Å, slightly different from GS structure before irradiation. This suggests again, that in the system the MS1 isomer is also present. In Ru1 complex only MS1 (population is 47%) and GS were found. Distances of GS are presented in Table S1. Ru1-O112 (MS1) = 1.78(1) Å, N112-O112 = 1.17(1) Å. Again, in case of non ~100% of state, MS1 and GS distances differ from data discussed in the previous GS and MS1 refinement sections. The population dependence of MS1 and GS distance changes was shown in[2]. To be sure, that after all irradiation procedures the system relaxes back to GS, the same crystal was heated up to room temperature and data were collected again after several days. Crystal data and selected distances/angles are shown in Tables S1, S2 and S3 and corresponds to the GS before irradiation bearing in mind, that data were collected at room temperature, but not at 100 K.

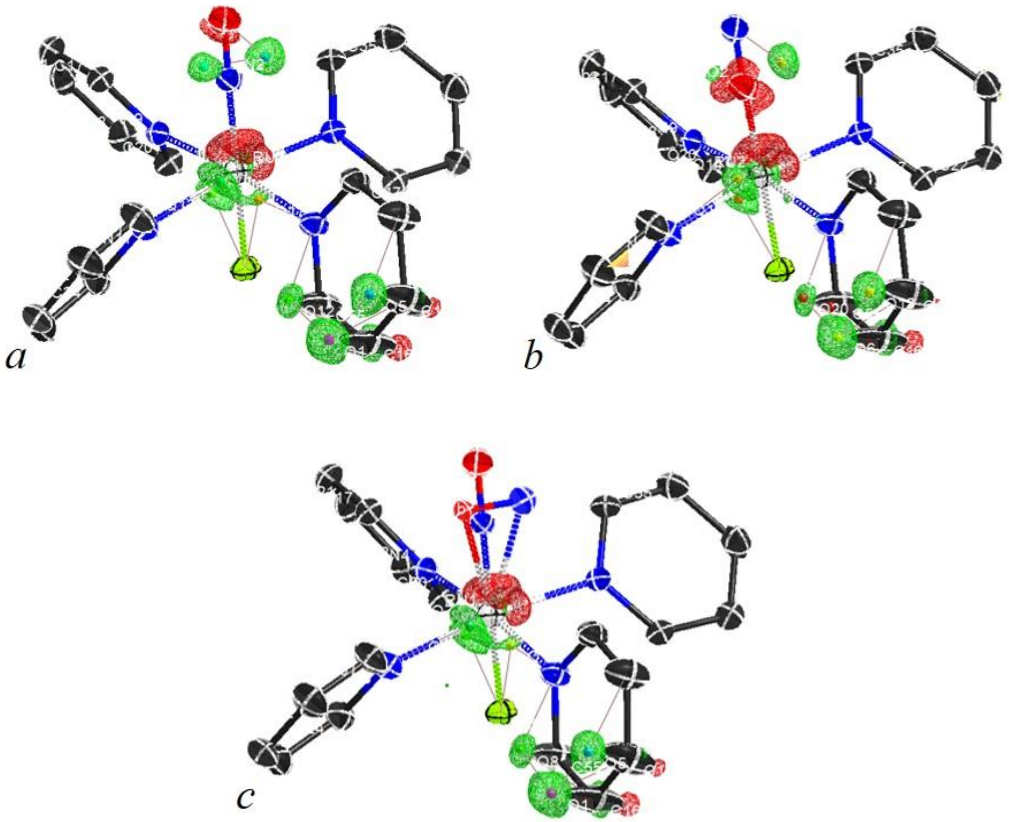

Figure S5. Residual electron density maps of structure refinement with Ru-NO (*a*, top, left), Ru-ON (*b*, top, right) groups and both Ru-NO and Ru-(η^2-(NO)) (*c*, bottom). Occupancy of Ru-(η^2-(NO)) isomer in the last model is 17%. Only Ru2 fragment is presented due to absence of MS2 isomer in Ru1 fragment. Excess of electrons are shown by the green color, depletion by the red color. The residual electron density surfaces are 0.4 eÅ^{-3}.

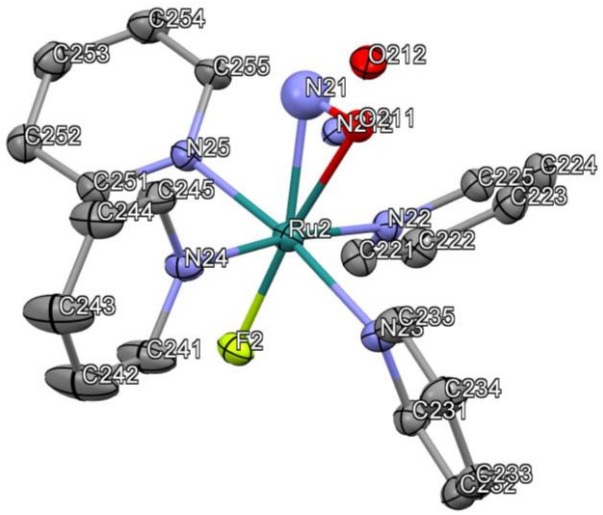

Figure S6. Structure of $[RuNOPy_4F](ClO_4)_2$ complex (Ru2 particle) refined with both Ru-NO and Ru-(η^2-(NO)) groups. Occupancy of Ru-(η^2-(NO)) isomer is 17%. Anions (ClO_4^-) and hydrogen atoms are omitted.

Spectroscopy studies

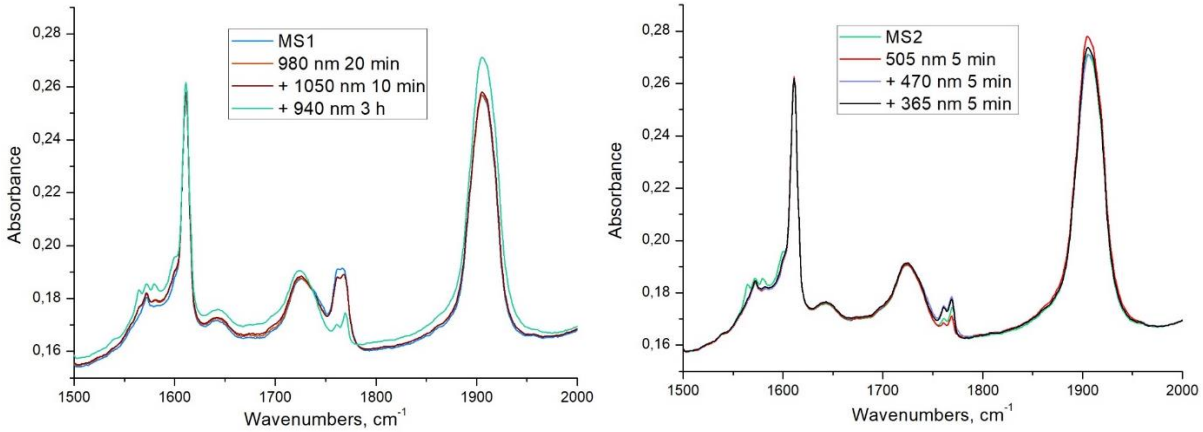

Figure S7. (left) IR spectra during MS1-MS2 transfer with infrared light: spectrum of MS1 (blue), after 20 min of 980 nm irradiation (orange), after 10 min of 1050 nm irradiation (brown), and after 3 h of 940 nm irradiation (green). (right) IR spectra during MS2-GS transfer: spectrum of MS2 (green), after 5 min of 505 nm irradiation (red), after 5 min of 470 nm irradiation (blue), and after 5 min of 365 nm irradiation (black).

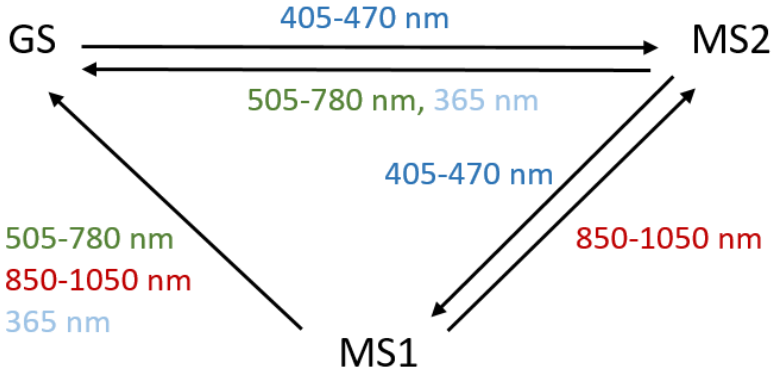

Figure S8. Scheme of linkage isomerization in $[RuNO(Py)_4F](ClO_4)_2$ indicating relevant spectral ranges for population and depopulation with light.

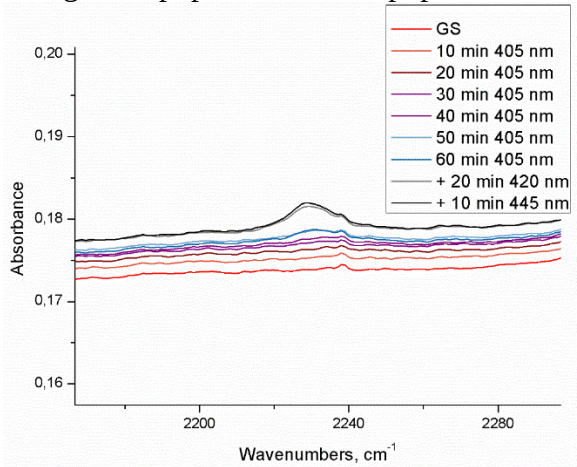

Figure S9. The band at 2230 cm^{-1}, which appears after more than 60 min irradiation by blue light. The band presumably corresponds to the frequency vibration of N_2O formed after the partial NO release from the $[RuNO(Py)_4F](ClO_4)_2$ complex.

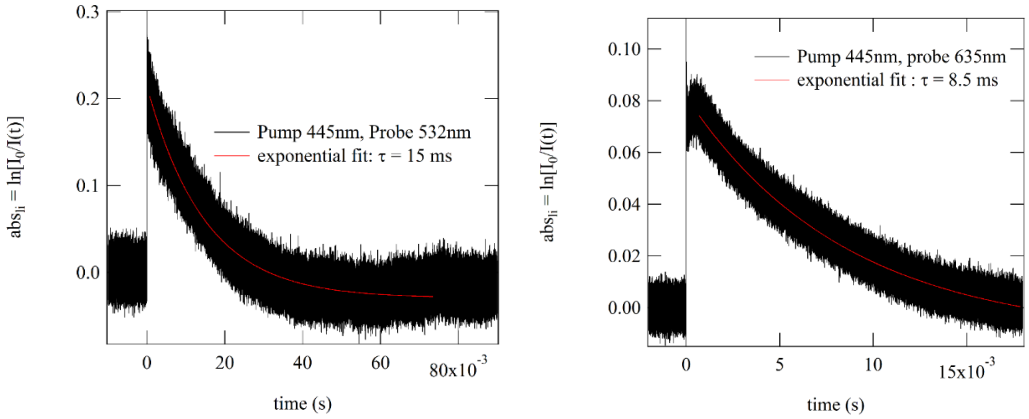

Figure S10. Absorption changes in $[RuNOPy_4F](ClO_4)_2$ single crystal after excitation with a 5ns LASER pulse at 445 nm and probing at 532 mn (left) and 635 nm (right). The experimental data is fitted by mono-exponential kinetic yielding lifetimes of 15 and 8.5 ms for the 532 and 635 nm probe wavelength, respectively.

References

[1] G. A. Kostin, A. A. Mikhailov, N. V Kuratieva, D. P. Pishchur, A. N. Makhinya, *New J. Chem.* **2018**, *42*, 18928–18934.

[2] B. Cormary, I. Malfant, M. Buron-Le Cointe, L. Toupet, B. Delley, D. Schaniel, N. Mockus, T. Woike, K. Fejfarová, V. Petříček, et al., *Acta Crystallogr. Sect. B Struct. Sci.* **2009**, *65*, 612–623.

[3] G. A. Kostin, A. O. Borodin, A. A. Mikhailov, N. V. Kuratieva, B. A. Kolesov, D. P. Pishchur, T. Woike, D. Schaniel, *Eur. J. Inorg. Chem.* **2015**, *29*, 4905–4913.

[4] G. A. Kostin, A. A. Mikhailov, N. V. Kuratieva, D. P. Pischur, D. O. Zharkov, I. R. Grin, *New J. Chem.* **2017**, *41*, 7758–7765.

[5] R. D. Yamaletdinov, I. L. Zilberberg, *Eur. J. Inorg. Chem.* **2017**, *23*, 2951–2954.